RESUSCITATION xxx (2026) xxx–xxx

Available online at ScienceDirect

Resuscitation

journal homepage: www.elsevier.com/locate/resuscitation

Original paper

MRI-based quantitative profiling of hypoxic-ischemic brain injury in postanoxic status epilepticus and other EEG patterns

Carlo Morotti Colleoni[a,b,*], *Urs Fisch*[b,c], *Samuel B. Snider*[d,e], *Benjamin A. Scirica*[e,f], *Matteo Pozzi*[g,h], *Gianmarco Carenini*[g,h], *Paolo Remida*[h,i], *Simone Beretta*[h,j], *Jong Woo Lee*[b,e]

Abstract

Aim: The pathophysiology and prognostic significance of postanoxic status epilepticus (SE) remain poorly defined. We compared the extent of hypoxic–ischemic brain injury (HIBI) in postanoxic SE with other EEG patterns, particularly generalized periodic discharges (GPDs), using quantitative MRI analysis.

Methods: Retrospective two-center observational study of consecutive comatose patients after cardiac arrest, having EEG and brain MRI data. Patients were classified into four EEG pattern groups (SE, GPDs, malignant, or benign). Quantitative ADC maps were compared across groups using region-of-interest and voxel-wise analyses. Secondary multivariable logistic models assessed predictors of neurological recovery (coma recovery at discharge and Cerebral Performance Category at 3 months).

Results: Among 192 postanoxic patients (76 benign, 46 GPDs, 44 malignant, 26 SE), coma recovery occurred in 30.7% and 21.2% achieved a CPC 1–2 at 3 months. Whole-brain ADC values differed significantly across EEG patterns ($p < 0.001$), with the lowest values in malignant patterns (median 750 $\times$ 10^{-6} mm^2/s) and GPDs (838 $\times$ 10^{-6} mm^2/s), and higher values in SE (893 $\times$ 10^{-6} mm^2/s) and benign patterns (907 $\times$ 10^{-6} mm^2/s; $p < 0.001$). SE showed significantly higher ADC than malignant ($p < 0.001$) and GPD groups ($p = 0.021$), but did not differ from the benign group ($p = 0.26$). Regional and voxel-wise analyses confirmed these findings. In multivariable models, higher occipital cortical ADC was an independent predictor of good outcome, alongside EEG pattern, clinical variables, and neuron-specific enolase.

Conclusions: Postanoxic SE exhibited a more favorable HIBI profile than GPDs or malignant EEG patterns.

Keywords: Post-anoxic status epilepticus, Neuroprognostication, Hypoxic–ischemic encephalopathy, Diffusion-weighted imaging (DWI), Generalized periodic discharges (GPDs), Heart arrest

Introduction

International guidelines recommend a multimodal approach for neurological prognostication after cardiac arrest.[1–4]

Specific EEG patterns are well established as markers of poor prognosis.[5,6] Postanoxic status epilepticus (SE) remains controversial with regard to outcome and treatment intensity.[7–9] Recent studies indicate that a subset of patients with post-cardiac arrest SE and no other unfavorable prognostic markers may achieve a favorable functional outcome, although robust evidence on treatment efficacy is lacking.[10–12]

Conventional brain MRI assessment remains qualitative and operator-dependent; the added value of quantitative approaches is still unsettled.[13] Quantitative mapping of the apparent diffusion coefficient (ADC) offers an objective, reproducible measure, potentially limiting inter-observer variability.[14–17]

We aimed to quantify the extent and regional distribution of MRI-defined hypoxic-ischemic brain injury (HIBI) using ADC metrics in patients resuscitated from cardiac arrest, comparing different EEG

* Corresponding author at: PhD program in Neuroscience, School of Medicine and Surgery, University of Milano-Bicocca, Monza, Italy, Via Cadore, 48, 20900, Monza (MB), Italy.

E-mail address: c.morotticolleoni@campus.unimib.it (C. Morotti Colleoni).

https://doi.org/10.1016/j.resuscitation.2026.111153

Received 13 January 2026; Received in Revised form 15 May 2026; Accepted 18 May 2026

Please cite this article as: C. Morotti Colleoni, U. Fisch, S.B. Snider et al., MRI-based quantitative profiling of hypoxic-ischemic brain injury in postanoxic status epilepticus and other EEG patterns, Resuscitation, https://doi.org/10.1016/j.resuscitation.2026.111153

patterns, focusing on SE. We hypothesized that patients with SE would exhibit less extensive HIBI compared to patients with malignant EEG features, such as a suppressed background or generalized periodic discharges (GPDs). A secondary aim was to combine quantitative ADC data with EEG patterns and clinical predictors to test a multimodal prognostic model for a favorable outcome.

Materials and methods

Study design

This retrospective observational study included post-cardiac arrest patients from two centers, Boston (USA), Monza (Italy) participating in the NEXT-CAT multicenter collaboration, ancillary of the SUPERCAT study (NCT05756621). The NEXT-CAT cohort comprised consecutive comatose patients undergoing EEG and NSE testing, identified through prospective registries and administrative data queries. The present study focused on the subset of patients who underwent brain MRI between 2012 and 2025.

Ethics

The study was approved by the local institutional review boards of the participating centers (MGB #2014P001623; SUPERCAT IRB: ID 4746_SA 26.O4.2024_M). In Boston, the requirement for informed consent was waived by the institutional review board. In Monza, informed consent was obtained from surviving participants, whereas consent was waived for deceased or unreachable participants.

Eligibility criteria

Adult cardiac arrest patients who were comatose (not awake and not obeying commands)[1] at 24 h, had at least one NSE measurement within 24–72 h, underwent continuous EEG monitoring within 72 h, and received brain MRI within 10 days were included.

Study outcomes and sample size

The primary outcome was the distribution of whole-brain ADC values across EEG patterns. Secondary outcomes were regional ADC distributions across EEG patterns and performance of a multimodal prognostic model for a favorable outcome.

We planned to compare ADC values, treated as continuous variables, across EEG patterns using the Kruskal–Wallis test. Assuming a medium effect size of 0.25 standard deviations, a total of 160 patients was needed to achieve 80% power at a significance level of 0.05 to detect differences in ADC values across the EEG groups.

Data collection

Clinical and demographic variables were extracted from medical records. Clinical outcomes were: recovery of consciousness at hospital discharge, defined as following commands; functional status at 3 months, assessed using the Cerebral Performance Category (CPC) scale (good outcome: CPC 1–2; poor outcome: CPC 3–5). The highest NSE value within 24–72 h was recorded; blood samples were screened for hemolysis according to each center's laboratory cut-offs.

EEG patterns

All patients underwent continuous EEG monitoring. In Boston a standard 19-channel montage was used, while a reduced 8-channel montage was adopted in Monza.[8] For each patient, a predominant EEG pattern was determined preferentially during normothermia and off sedation, considering the recordings from the first 5 days following cardiac arrest. Recordings under sedation or hypothermia were used only when no other recordings were available.

A modified version, incorporating the Beretta[8] and the Westhall classifications,[6] was used for EEG categorization in four mutually exclusive EEG patterns:

- GPDs, defined according to the American Clinical Neurophysiology Society (ACNS) terminology[18] as GPDs not fulfilling criteria for SE, irrespective of the presence of motor manifestations.
- SE, defined according to the Salzburg criteria,[19] either convulsive or non-convulsive.
- Malignant, defined as suppressed or burst-suppressed background (<10 μV) or low-voltage background (10–20 μV), corresponding to the Westhall "highly malignant" category, but in the absence of GPDs or SE at any time point.
- Benign, defined as a residual category, by the absence of malignant features, GPDs, or SE at any time point. This group may include interictal epileptiform discharges in the context of continuous background, but not SE, seizures or GPDs.

To avoid overlap between categories and to allow a separate identification of patients with SE in the absence of GPDs, a predefined hierarchical approach was adopted, consistent with the methodological framework previously implemented.[8] In this scheme, GPDs were prioritized; if absent, SE was assigned, then malignant pattern; cases not meeting any prior category were classified as benign (Supplementary Fig. 1A). Classification was based on the predominant EEG pattern across the available recordings.

Background continuity was dichotomized as continuous (including nearly continuous) or non-continuous (from discontinuous to suppressed) (Supplementary Fig. 1B). EEG patterns and background classification followed the standardized ACNS terminology[18] and were assessed independently by local neurophysiologists.

Post-cardiac arrest management

Post-cardiac arrest patients were managed according to international guidelines for post-resuscitation care and neurological prognostication, which evolved over the study period.[1,20–23] The management of epileptiform patterns, including SE, followed guideline recommendations and local practice.[1,8,23,24] Initial treatment generally included intravenous levetiracetam or sodium valproate, with addition of sedative agents when indicated. For refractory SE, second-line antiseizure medications or anesthetic agents were used according to local protocols.[8]

MRI analysis

T1-weighted images were segmented using FreeSurfer SynthSeg.[25] ADC maps were co-registered to T1-weighted images with FSL (Oxford Center for Functional MRI of the Brain) using nearest-neighbor interpolation.[26] Automated registrations were visually inspected for accuracy.

Mean ADC values were extracted from each anatomical region of interest (ROI) defined by SynthSeg, either directly or after combining labels.[27] To exclude artifacts and cerebrospinal fluid, only values between 200 and 2000 $\times$ 10^{-6} mm^2/s were considered.[17] Whole-brain and supratentorial cortical ADC values were also extracted for subgroup comparisons. To corroborate the ROI-based analyses, a voxel-based lesion-symptom mapping analysis was performed using FSL PALM (Permutation Analysis of Linear Models).[28] T1-weighted and ADC images were co-registered to MNI space with

Freesurfer EasyReg.[29] Design and contrast matrices were created to run two-sample permutation *t*-tests (2000 permutations), comparing EEG subgroups pairwise, with and without covariates (age, presenting pulseless rhythm), using threshold-free cluster enhancement (TFCE).[30] Because no universally accepted ADC threshold exists to define tissue infarction after cardiac arrest, ADC was analyzed as a continuous variable, as previously reported.[14,15,31] Each EEG subgroup was also compared with healthy controls available from a previous study,[31] to confirm inter-pattern robustness.

Statistical analysis

Variables were summarized using standard descriptive statistics and differences across EEG patterns were assessed using appropriate tests. Since ADC values were non-normally distributed, the Kruskal-Wallis test with false discovery rate-adjusted pairwise analyses was used.[32] An aligned rank transform (ART) ANOVA evaluated the effects of background continuity in SE and GPD subgroups. Prognostic performance for coma recovery and 3-month outcome (CPC 1–2 vs 3–5) was assessed using two modeling strategies. A multivariable logistic regression with backward stepwise elimination (BIC criterion) and a penalized logistic regression using LASSO regularization, both incorporating clinical, EEG, serum NSE (log-transformed) and a literature-based selection of quantitative ADC predictors. As a sensitivity analysis, targeted temperature management (TTM) was added as an additional predictor in the penalized models, as a surrogate marker of post-resuscitation care, and all prognostic models were repeated after excluding patients who recovered command-following within 72 h after cardiac arrest. Model discrimination was assessed by receiver operating characteristic (ROC) analysis, with area under the curve (AUC) and Brier score estimated through nested 5 × 5 stratified cross-validation. To ensure robustness, 1000-iteration bootstrap resampling was used to derive confidence intervals, evaluate calibration (slope, intercept), and assess variable stability based on LASSO selection frequency. Analyses were conducted in R (version 4.5.0).

Data availability

Access to anonymized data is available from the corresponding author upon reasonable request, contingent on approval by the local institutional review boards.

Results

Characteristics of the study population

Baseline characteristics are shown in Table 1.

Complete MRI data were available for 197 patients (142 from Boston and 55 from Monza). A total of 5 patients were excluded due to major structural abnormalities, leaving 192 patients for the final analysis (Supplementary Fig. 2). 49 healthy controls were included as reference.

Median age was similar across the EEG groups ($p = 0.665$), with a male predominance (66.7%). Shockable rhythms occurred in 47.9% of patients, less frequently in the malignant group (25.0%; $p = 0.007$). NSE concentrations differed significantly across the four EEG patterns, with higher median values in malignant (128.0 [78.0–275.2] ng/mL) and GPD (84.0 [46.5–213.0] ng/mL) groups compared with benign (28.0 [18.0–45.0] ng/mL) and SE (40.9 [21.0–49.9] ng/mL) patients ($p < 0.001$). Moreover, a continuous background was observed more frequently in SE (73.1%) than in GPDs (39.1%; $p = 0.007$).

In-hospital mortality was 59.9% (115/192). Most deaths (103/115, 89.6%) occurred following withdrawal of life-sustaining therapy (WLST) due to presumed poor neurological prognosis (Supplementary Table 1). Overall, 59 patients recovered consciousness by hospital discharge, while 38 achieved a CPC of 1–2 at 3 months. Fourteen patients (7.3%) recovered command-following within 72 h after cardiac arrest; all belonged to the benign EEG group and most had favorable outcomes. Malignant and GPD patterns were invariably associated with poor prognosis, while patients with SE had intermediate outcomes compared with the benign pattern group, both for coma recovery at discharge (31% versus 64.5%, respectively; $p < 0.001$) and functional outcome at 3 months (22% versus 49%, respectively; $p < 0.001$).

Quantitative ADC values according to the EEG patterns

In the overall cohort, the median whole-brain ADC was 874 × 10^{-6} mm^2/s (IQR 802–930). Across the four EEG patterns, whole-brain and regional ADC values differed significantly (Kruskal–Wallis $p < 0.001$), with the lowest values in malignant and GPD patterns and higher values in SE and benign groups (Table 2, Fig. 1).

Post-hoc analyses confirmed that SE differed markedly from malignant (893 [IQR 855–935] × 10^{-6} mm^2/s versus 750 [IQR 701–804] × 10^{-6} mm^2/s, respectively; $p < 0.001$) and was not significantly different from benign (907 [IQR 873–951] × 10^{-6} mm^2/s; $p = 0.26$). Whole-brain ADC values in SE were significantly higher than in GPDs (838 [IQR 779–915] × 10^{-6} mm^2/s; $p = 0.021$). Similar results were obtained for supratentorial cortical ADC values. Associations between EEG patterns and ADC values were consistent across both centers.

In the subgroup of patients with SE and GPDs, a two-way ART-ANOVA revealed significant main effects of both EEG category and background activity on whole-brain and cortical ADC values (whole-brain: EEG category $p = 0.023$, background activity $p = 0.044$; cortical ADC: EEG category $p = 0.026$, background activity $p = 0.037$), with no significant interaction between factors (whole-brain $p = 0.367$; cortical ADC $p = 0.309$) (Supplementary Fig. 3). However, in stratified Wilcoxon analyses, background continuity was not associated with significant ADC differences within the SE subgroup (whole-brain $p = 0.91$; cortical ADC $p = 0.91$), while a non-significant trend toward higher ADC values was observed among GPD patients with a continuous background (whole brain $p = 0.142$; cortical ADC $p = 0.124$; median 847.9 [817.7–930.0] vs 833.8 [720.7–899.9] × 10^{-6} mm^2/s).

Voxel-wise permutation testing with PALM corroborated the ROI-based results. Malignant EEG patterns showed widespread clusters of significantly reduced ADC values compared with benign and SE groups, while GPDs displayed intermediate reductions (TFCE, FDR-corrected $p < 0.05$). ADC values in SE did not significantly differ from the benign EEG pattern. These findings remained consistent after adjustment for age and presentation rhythm (Fig. 2). Compared with healthy controls, malignant and GPD patterns showed extensive cortical and subcortical ADC reductions (TFCE, FDR-corrected $p < 0.05$), whereas SE and benign patterns did not (Supplementary Fig. 4).

Table 1 – Baseline characteristics and main clinical outcomes of the study population.

	All patients (*N* = 192)	Benign (*n* = 76)	Malignant (*n* = 44)	GPDs (*n* = 46)	SE (*n* = 26)	*p* value
Age, years	62.5 [52.5–71.2]	62.0 [50.5–75.0]	64.5 [55.0–73.0]	60.0 [50.2–67.8]	66.5 [54.8–70.0]	0.665
Sex, male	128 (66.7%)	54 (71.1%)	32 (72.7%)	28 (60.9%)	14 (53.8%)	0.261
Shockable presentation rhythm	92 (47.9%)	43 (56.6%)	11 (25.0%)	24 (52.2%)	14 (53.8%)	0.007
OHCA	150 (78.1%)	51 (67.1%)	36 (81.8%)	41 (89.1%)	22 (84.6%)	**0.022**
ROSC, min	21.0 [11.0–30.0] (*n* = 133/192)	20.0 [9.5–28.5]	24.5 [15.0–43.8]	21.5 [15.3–30.0]	23.0 [10.0–30.0]	0.236
Targeted temperature management	132 (68.8%)	53 (69.7%)	24 (54.5%)	33 (71.7%)	22 (84.6%)	0.060
Neuron-specific Enolase, ng/mL	49.4 [26.9–110.0]	28.0 [18.0–45.0]	128.0 [78.0–275.2]	84.0 [46.5–213.0]	40.9 [21.0–49.9]	**<0.001**
Continuous background activity*	–	–	–	18 (39.1%)	19 (73.1%)	**0.007**
Interval from cardiac arrest to MRI (days)	4.0 [3.0–6.0]	4.0 [3.0–7.0]	3.0 [2.0–4.0]	3.5 [2.0–4.0]	4.5 [3.0–7.8]	**<0.001**
In-hospital mortality	115 (59.9%)	20 (26.3%)	40 (90.9%)	42 (91.3%)	13 (50.0%)	**<0.001**
Coma recovery at discharge	59 (30.7%)	49 (64.5%)	1 (2.3%)	1 (2.2%)	8 (30.8%)	**<0.001**
Good functional outcome at 3 months (CPC 1–2)	38/179 (21.2%)	33 (49.3%)	0 (0%)	0 (0%)	5 (21.7%)	**<0.001**

Abbreviations: OHCA, out-of-hospital cardiac arrest; ROSC, return of spontaneous circulation; CPC, Cerebral Performance Category.
Values are median [IQR] or *n* (%). *P* values were obtained using Kruskal–Wallis or Fisher's exact tests, as appropriate.
* Data available only for patients with status epilepticus and GPD patterns.

Table 2 – Median ADC values across EEG categories for selected brain regions of interest (ROI).

	All patients (*N* = 192)	Benign (*n* = 76)	SE (*n* = 26)	GPDs (*n* = 46)	Malignant (*n* = 44)	*p*-value
Whole brain	874 [802–930]	907 [873–951]	893 [855–935]	838 [779–915]	750 [701–804]	**<0.001**
Supratentorial cortex	946 [856–1024]	993 [943–1044]	974 [933–1025]	899 [834–1011]	788 [717–887]	**<0.001**
Basal ganglia	821 [764–867]	853 [825–884]	846 [812–875]	812 [774–854]	755 [723–792]	**<0.001**
Thalamus	863 [824–906]	871 [840–902]	863 [833–891]	824 [782–868]	762 [730–806]	**<0.001**
Postcentral gyrus	983 [857–1065]	1040 [981–1098]	1010 [957–1070]	924 [810–1077]	817 [669–937]	**<0.001**
Occipital cortex	927 [768–1039]	1004 [927–1082]	985 [893–1051]	847 [703–969]	723 [653–807]	**<0.001**

Values are expressed as median (interquartile range); ADC values are reported in $\times 10^{-6}$ mm^2/s; regions of interest (ROIs) refer to bilateral structures; *p*-values refer to overall group differences assessed by the Kruskal–Wallis test.

Predictive models

In backward stepwise logistic regression, independent predictors of coma recovery included age, presentation rhythm, serum NSE levels (lower values being associated with better outcomes), EEG pattern and background (with GPDs and malignant features negatively associated), regional ADC, particularly in the occipital cortex and basal ganglia. The model achieved a cross-validated AUC of 0.86 (95% CI 0.73–0.94), sensitivity 0.92, and specificity 0.79, with modest calibration (slope 0.56; intercept −0.12) (Fig. 3, Supplementary Table 2).

Penalized logistic regression with LASSO regularization yielded comparable results (AUC 0.88, 95% CI 0.79–0.93; sensitivity 0.92, specificity 0.82), selecting the same stable predictors and showing better calibration (slope 0.84; intercept near zero).

When applied to 3-month functional outcome (CPC 1–2 vs 3–5, *n* = 179), both models maintained similar discrimination and calibration (Table 3), confirming the robustness of prognostic determinants over time.

Including TTM or excluding patients who recovered command-following within 72 h did not materially change model performance or the most stable predictors for either outcome.

Discussion

This study demonstrates that post-anoxic SE exhibits a less extensive quantitative MRI-defined HIBI than malignant features such as

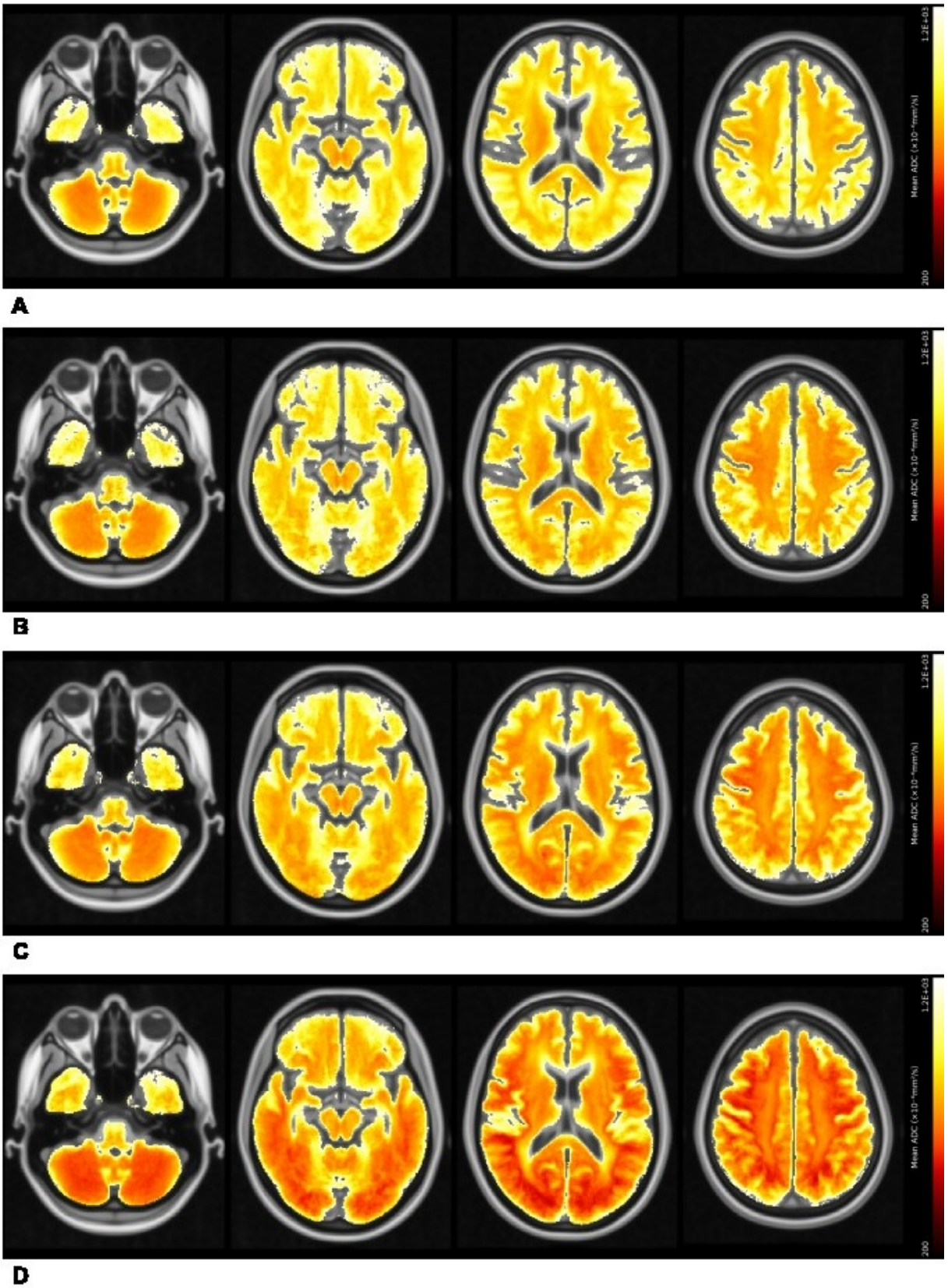

Fig. 1 – Mean apparent diffusion coefficient (ADC) maps across EEG categories.
Panels illustrate mean ADC maps for patients grouped according to the EEG pattern, co-registered to the MNI152 T1 template. Panels represent benign group (**A**), status epilepticus (**B**), GPDs (**C**) and malignant EEG pattern (**D**). Darker areas indicate lower ADC values, as shown by the color bar on the right.

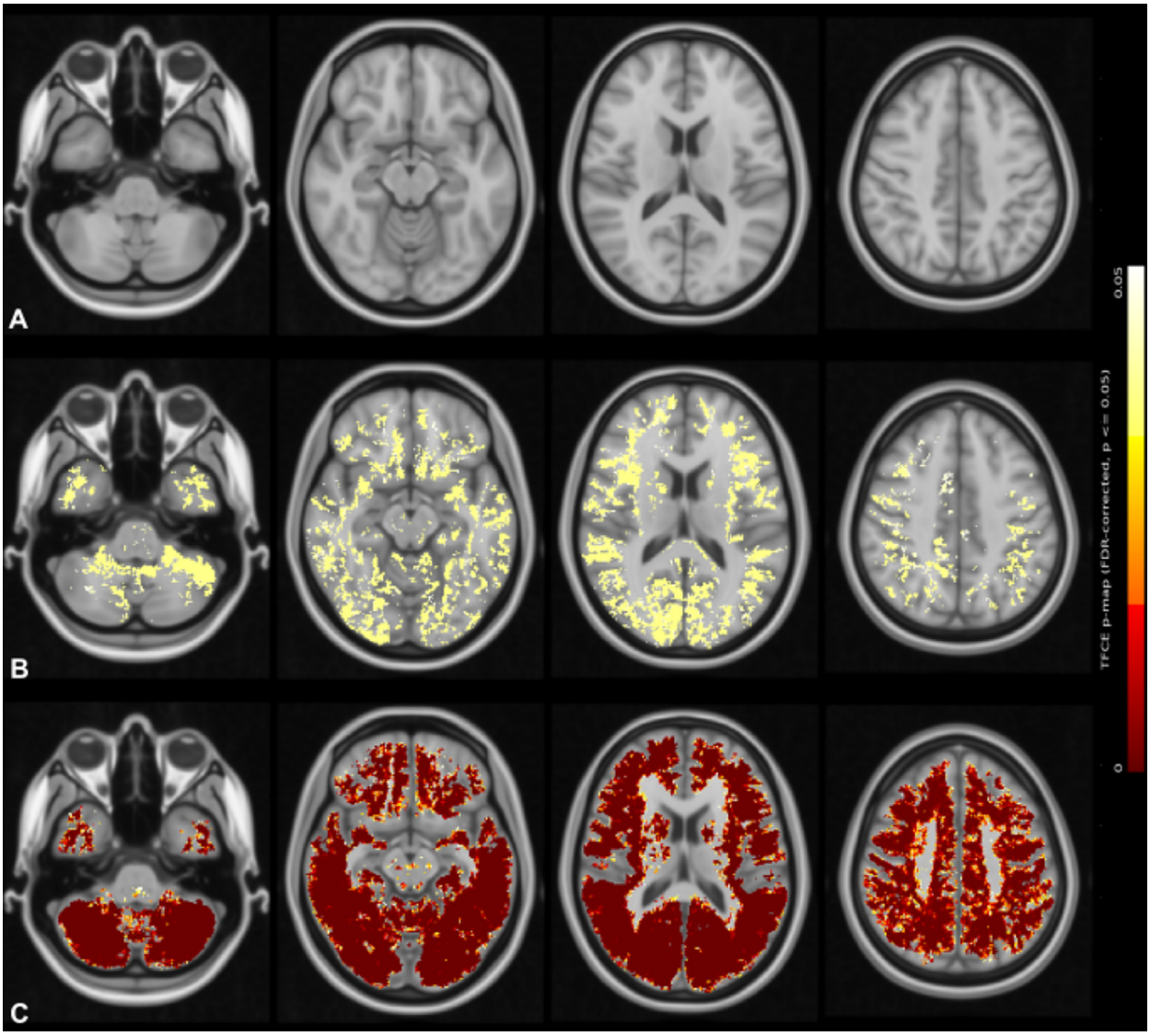

Fig. 2 – PALM analysis of ADC differences between status epilepticus and other EEG categories.
Permutation Analysis of Linear Models (PALM) showing voxel-wise differences in ADC values between status epilepticus and the other EEG patterns: benign (panel **A**), GPDs (panel **B**), and malignant (panel **C**), corrected for confounders. Clusters with significant FDR-corrected differences ($p < 0.05$) are overlaid on the MNI152 T1 template.

GPDs and closely resembles the degree and distribution seen in benign EEG patterns.

These findings may reflect underlying pathophysiology. In the context of HIBI, more severe and diffuse damage may limit the generation of sustained epileptiform activity, whereas SE may indicate partially preserved cortical function.[33] In contrast, GPDs could be associated with more severe cortical injury.[31,33–35]

In our cohort, ADC values in SE did not differ significantly from benign patterns or in healthy controls; therefore, SE may still be compatible with a favorable outcome in the early post-arrest phase.[10,11]

Loss of background continuity is generally considered a marker of poor neurological prognosis after cardiac arrest.[36,37] In our cohort, however, no clear relationship between absent background continuity and HIBI severity was observed among SE patients. Our findings suggest that SE may be considered a prognostic category of its own, independent of background continuity. This conclusion, however, reflects the eligibility criteria of our study, which excluded two severe epileptiform conditions from the SE group: patients who progressed to GPDs with suppressed background (classified as "GPDs" in our study)[38]; and patients with clinical myoclonus but burst suppression with highly epileptiform bursts (classified as "malignant").[6,39] Despite these limitations, the pragmatic classification used here remains clinically useful and may help design future studies on postanoxic SE.

Within the GPD cohort, the wide range of ADC values indicates substantial heterogeneity in HIBI. Stratification by background continuity showed a nonsignificant trend toward higher ADC values in patients with continuous background may suggest a distinct, potentially less severe phenotype, likely reflecting triphasic waves of metabolic encephalopathy.[40,41] These findings suggest that GPDs encompass a spectrum of conditions not fully captured by background continuity alone, warranting caution in early prognostic interpretation.

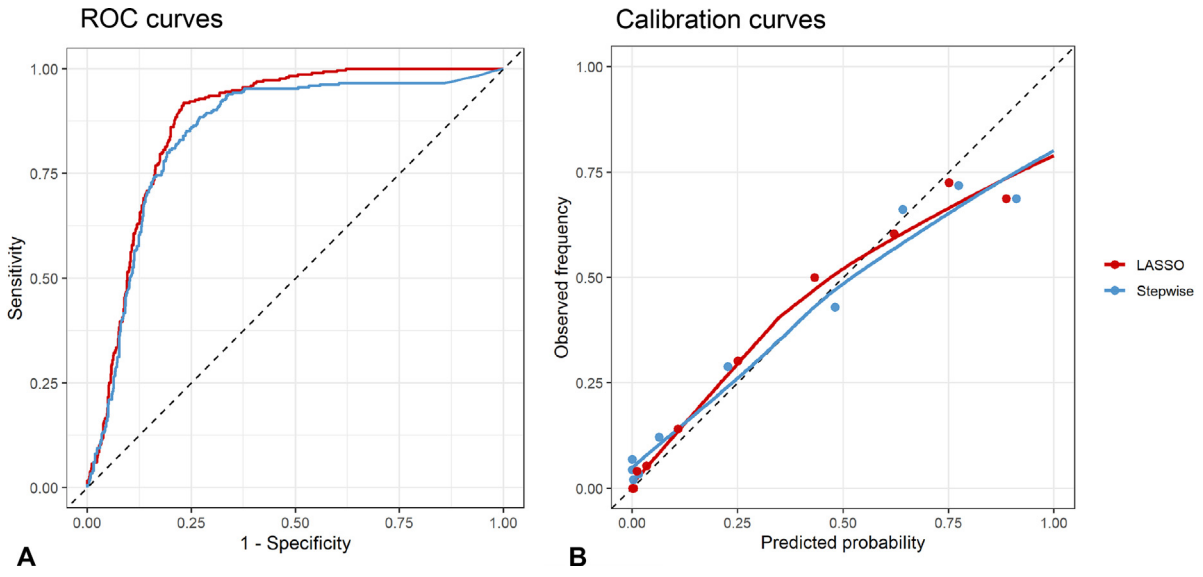

Fig. 3 – Performance of stepwise and LASSO regression models for coma recovery prediction.
(**A**) Out-of-bag receiver operating characteristic (ROC) curves comparing discrimination performance of the stepwise (blue) and LASSO (red) logistic regression models. (**B**) Calibration plots showing the agreement between predicted and observed probabilities for both models, after bootstrap correction. The dashed line indicates perfect calibration. (For interpretation of the references to color in this figure legend, the reader is referred to the web version of this article.)

Table 3 – Comparison of performance metrics between stepwise and LASSO logistic regression models for good outcome prediction.

	Coma recovery		CPC 1–2 at 3 months	
Metric	**Stepwise regression**	**LASSO regression**	**Stepwise regression**	**LASSO regression**
AUC	0.86	0.88	0.86	0.90
Brier score	0.144 (95% CI 0.096–0.238)	0.138 (95% CI 0.103–0.223)	0.134 (95% CI 0.092–0.166)	0.116 (95% CI 0.067–0.153)
Calibration slope	0.56 (95% CI 0.14–1.43)	0.84 (95% CI 0.30–1.40)	0.39 (95% CI 0.21–0.84)	0.78 (95% CI 0.43–1.46)
Calibration intercept	−0.12 (95% CI −0.64 to 0.18)	−0.04 (95% CI −0.50 to 0.47)	−0.21 (95% CI −0.60 to 0.39)	−0.13 (95% CI −0.68 to 0.43)
Sensitivity (Youden pooled)	0.92	0.92	0.96	0.99
Specificity (Youden pooled)	0.79	0.82	0.69	0.62

AUC values were estimated from nested cross-validation, whereas calibration slope and intercept were derived from bootstrap resampling.

The predictive models for good outcome retained validated biomarkers such as NSE[42–44] and confirmed the prognostic value of age and initial rhythm.[45,46] Background continuity remained a key determinant of outcome.[37] Malignant EEG features and GPDs were associated with poor prognosis, whereas SE showed a weaker association, supporting our EEG classification. These results align with a post-hoc analysis of the TELSTAR trial, which suggested potential benefit of aggressive SE treatment but no benefit in GPDs.[12] However, this finding should be interpreted in the context of a high proportion of deaths following WLST for presumed poor neurological prognosis, particularly in patients with malignant EEG patterns and GPDs, which may introduce a self-fulfilling prophecy bias.[47] Inter-center variability in CPC assessment should also be considered.

When regional mean ADC values were included in the models, only a limited number of regions remained significant, primarily within the occipital cortex. Higher ADC values in this area were associated with better outcome. As a metabolically active and hypoxia-sensitive cortical region, relative preservation of the occipital cortex likely indicates less severe global injury and a more favorable prognosis.[31,48]

The basal ganglia, another region frequently affected in HIBI, were only weakly retained in our models, suggesting limited prognostic value compared with cortical structures. Although ADC values in the postcentral gyrus have previously been associated with favorable

outcome,[14] our models did not highlight this region, possibly reflecting differences in cohort size or population characteristics.

Limitations

Although our predictive model supported the robustness of the proposed EEG classification, we recognize that our approach differs from the categorization most commonly adopted in prior studies,[6] with a limited risk of misclassification due to very early transient EEG patterns. Our decision to analyze SE separately from malignant patterns, including GPDs, was motivated by emerging evidence that, particularly in the absence of additional unfavorable indicators, SE may still be compatible with meaningful recovery.[8,10,11] Accordingly, a good 3-month functional outcome was observed in >20% of patients with SE, consistent with recent data.[11]

MRI timing differed among EEG categories, with earlier imaging in GPD and malignant. However, the median delay across all subgroups remained within the optimal sensitivity window for DWI detection of HIBI.[3,16] Earlier MRI in malignant patients likely reflects the clinical need for faster neuroprognostication in those with multiple unfavorable predictors.

EEG acquisition differed between centers; one site used a reduced 8-channel montage, limiting spatial resolution but unlikely to affect classification of generalized patterns.[49]

The long inclusion period spans changes in post–cardiac arrest care, including treatment of epileptiform patterns, and neuroprognostication, which may have influenced early neurological assessment. MRI availability may have affected patient selection. In addition, inclusion required multimodal testing, possibly introducing selection bias by excluding patients with early recovery or very poor prognosis.

Quantitative ADC analysis reduces operator-dependent interpretation but may be affected by artefactual distortions that could bias results. Its superiority over conventional qualitative assessment remains uncertain[13] and proposed prognostic ADC cut-offs often come from small, single-center studies with limited validation. Scanner heterogeneity across sites may also have influenced image processing and results, though prior studies have not confirmed this.[31] Larger studies are needed to confirm these findings.

Conclusions

Our study indicates that patients with postanoxic SE exhibit a more favorable HIBI profile, in terms of ADC values, than those presenting malignant EEG features or GPDs. These findings suggest that SE may be associated with distinct prognostic implications and underline the need for further studies to clarify its prognostic value and the optimal treatment strategies.

Funding statement

Carlo Morotti Colleoni was supported by grants from the Research Fund of the University of Milano-Bicocca.

Urs Fisch was supported by research grants from the Gottfried Julia Bangerter-Rhyner Foundation, the Andre and Michel Bouriez Foundation, and by grants from the Research Fund of the University of Basel.

CRediT authorship contribution statement

Carlo Morotti Colleoni: Writing – original draft, Visualization, Investigation, Formal analysis, Data curation. **Urs Fisch:** Writing – review & editing, Software, Methodology. **Samuel B. Snider:** Writing – review & editing, Software. **Benjamin A. Scirica:** Writing – review & editing. **Matteo Pozzi:** Writing – review & editing, Data curation. **Gianmarco Carenini:** Writing – review & editing. **Paolo Remida:** Writing – review & editing. **Simone Beretta:** Writing – original draft, Supervision, Conceptualization. **Jong Woo Lee:** Writing – original draft, Supervision, Resources, Formal analysis, Data curation, Conceptualization.

Declaration of competing interest

The authors declare no competing interests.

Appendix A. Supplementary material

Supplementary material to this article can be found online at https://doi.org/10.1016/j.resuscitation.2026.111153.

Author details

[a]PhD Program in Neuroscience, School of Medicine and Surgery, University of Milano-Bicocca, Monza, Italy[b]Department of Neurology, Brigham and Women's Hospital, Boston, MA, USA [c]Department of Neurology, University Hospital Basel, Basel, Switzerland[d]Division of Neurocritical Care, Department of Neurology, Brigham and Women's Hospital, Boston, MA, USA [e]Harvard Medical School, Boston, MA, USA [f]Department of Medicine, Division of Cardiology, Brigham and Women's Hospital, Boston, MA, USA[g]Department of Emergency and Intensive Care, Fondazione IRCCS San Gerardo dei Tintori, Monza, Italy [h]Department of Medicine and Surgery, University of Milano-Bicocca, Monza, Italy[i]Department of Radiology, Fondazione IRCCS San Gerardo dei Tintori, Monza, Italy[j]Department of Neurology and Stroke Unit, Fondazione IRCCS San Gerardo dei Tintori, Monza, Italy

REFERENCES

1. Nolan JP, Sandroni C, Cariou A, et al. European Resuscitation Council and European Society of Intensive Care Medicine guidelines 2025: post-resuscitation care. Intensive Care Med 2025;51:2213–88. https://doi.org/10.1007/s00134-025-08117-3.
2. Rajajee V, Muehlschlegel S, Wartenberg KE, et al. Guidelines for neuroprognostication in comatose adult survivors of cardiac arrest. Neurocrit Care 2023;38:533–63. https://doi.org/10.1007/s12028-023-01688-3.
3. Berg KM, Bray JE, Ng KC, et al. 2023 international consensus on cardiopulmonary resuscitation and emergency cardiovascular care science with treatment recommendations: summary from the Basic Life Support; Advanced Life Support; Pediatric Life Support; Neonatal Life Support; Education, Implementation, and Teams; and First Aid Task Forces. Circulation 2023;148:e187–280. https://doi.org/10.1161/CIR.0000000000001179.

4. Sandroni C, D'Arrigo S, Nolan JP. Prognostication after cardiac arrest. Crit Care 2018;22:150. https://doi.org/10.1186/s13054-018-2060-7.
5. Backman S, Cronberg T, Friberg H, et al. Highly malignant routine EEG predicts poor prognosis after cardiac arrest in the target temperature management trial. Resuscitation 2018;131:24–8. https://doi.org/10.1016/j.resuscitation.2018.07.024.
6. Westhall E, Rossetti AO, van Rootselaar AF, et al. Standardized EEG interpretation accurately predicts prognosis after cardiac arrest. Neurology 2016;86:1482–90. https://doi.org/10.1212/WNL.0000000000002462.
7. Rossetti AO, Logroscino G, Liaudet L, et al. Status epilepticus: an independent outcome predictor after cerebral anoxia. Neurology 2007;69:255–60. https://doi.org/10.1212/01.wnl.0000265819.36639.e0.
8. Beretta S, Coppo A, Bianchi E, et al. Neurologic outcome of postanoxic refractory status epilepticus after aggressive treatment. Neurology 2018;91:e2153–62. https://doi.org/10.1212/WNL.0000000000006615.
9. Barbella G, Lee JW, Alvarez V, et al. Prediction of regaining consciousness despite an early epileptiform EEG after cardiac arrest. Neurology 2020:94. https://doi.org/10.1212/WNL.0000000000009283.
10. Admiraal MM, Backman S, Annborn M, et al. Electrographic and clinical determinants of good outcome after postanoxic status epilepticus. Neurology 2025;104:e210304. https://doi.org/10.1212/WNL.0000000000210304.
11. De Stefano P, Hofmeijer J, Quintard H, et al. Features, outcome, and treatment of postanoxic status epilepticus: pooled analysis of 3 cohorts. Neurology 2025;105:e213913. https://doi.org/10.1212/WNL.0000000000213913.
12. Ruijter BJ, Keijzer HM, Tjepkema-Cloostermans MC, et al. Treating rhythmic and periodic EEG patterns in comatose survivors of cardiac arrest. N Engl J Med 2022;386:724–34. https://doi.org/10.1056/NEJMoa2115998.
13. Van Roy S, Hsu L, Ho J, et al. Quantitative and radiological assessment of post-cardiac-arrest comatose patients with diffusion-weighted magnetic resonance imaging. Neurocrit Care 2025;42:541–50. https://doi.org/10.1007/s12028-024-02087-y.
14. Wouters A, Scheldeman L, Plessers S, et al. Added value of quantitative apparent diffusion coefficient values for neuroprognostication after cardiac arrest. Neurology 2021:96. https://doi.org/10.1212/WNL.0000000000011991.
15. Yoon JA, Kang C, Park JS, et al. Quantitative analysis of early apparent diffusion coefficient values from MRIs for predicting neurological prognosis in survivors of out-of-hospital cardiac arrest: an observational study. Crit Care 2023;27:407. https://doi.org/10.1186/s13054-023-04696-z.
16. Hirsch KG, Fischbein N, Mlynash M, et al. Prognostic value of diffusion-weighted MRI for post-cardiac arrest coma. Neurology 2020:94. https://doi.org/10.1212/WNL.0000000000009289.
17. Hirsch KG, Mlynash M, Eyngorn I, et al. Multi-center study of diffusion-weighted imaging in coma after cardiac arrest. Neurocrit Care 2016;24:82–9. https://doi.org/10.1007/s12028-015-0179-9.
18. Hirsch LJ, Fong MWK, Leitinger M, et al. American Clinical Neurophysiology Society's standardized critical care EEG terminology: 2021 version. J Clin Neurophysiol 2021;38:1–29. https://doi.org/10.1097/WNP.0000000000000806.
19. Beniczky S, Hirsch LJ, Kaplan PW, et al. Unified EEG terminology and criteria for nonconvulsive status epilepticus. Epilepsia 2013;54:28–9. https://doi.org/10.1111/epi.12270.
20. Sandroni C, Cariou A, Cavallaro F, et al. Prognostication in comatose survivors of cardiac arrest: an advisory statement from the European Resuscitation Council and the European Society of Intensive Care Medicine. Resuscitation 2014;85:1779–89. https://doi.org/10.1016/j.resuscitation.2014.08.011.
21. Callaway CW, Donnino MW, Fink EL, et al. Part 8: post-cardiac arrest care: 2015 American Heart Association guidelines update for cardiopulmonary resuscitation and emergency cardiovascular care. Circulation 2015;132:S465–82. https://doi.org/10.1161/CIR.0000000000000262.
22. Nolan JP, Sandroni C, Böttiger BW, et al. European Resuscitation Council and European Society of Intensive Care Medicine guidelines 2021: post-resuscitation care. Intensive Care Med 2021;47:369–421. https://doi.org/10.1007/s00134-021-06368-4.
23. Hirsch KG, Amorim E, Coppler PJ, et al. Part 11: post-cardiac arrest care: 2025 American Heart Association guidelines for cardiopulmonary resuscitation and emergency cardiovascular care. Circulation 2025;152:S673–718. https://doi.org/10.1161/CIR.0000000000001375.
24. Brophy GM, Bell R, Claassen J, et al. Guidelines for the evaluation and management of status epilepticus. Neurocrit Care 2012;17:3–23. https://doi.org/10.1007/s12028-012-9695-z.
25. Billot B, Greve DN, Puonti O, et al. SynthSeg: segmentation of brain MRI scans of any contrast and resolution without retraining. Med Image Anal 2023;86:102789. https://doi.org/10.1016/j.media.2023.102789.
26. Jenkinson M, Smith S. A global optimisation method for robust affine registration of brain images. Med Image Anal 2001;5:143–56. https://doi.org/10.1016/s1361-8415(01)00036-6.
27. Fisch U, Breedlove K, Scirica BM, Snider SB, Lee JW, Lin AP. Utility of magnetic resonance spectroscopy in predicting favorable outcome in adult comatose patients following cardiac arrest. Resuscitation 2025;215:110700. https://doi.org/10.1016/j.resuscitation.2025.110700.
28. Winkler AM, Ridgway GR, Webster MA, Smith SM, Nichols TE. Permutation inference for the general linear model. Neuroimage 2014;92:381–97. https://doi.org/10.1016/j.neuroimage.2014.01.060.
29. Iglesias JE. A ready-to-use machine learning tool for symmetric multi-modality registration of brain MRI. Sci Rep 2023;13:6657. https://doi.org/10.1038/s41598-023-33781-0.
30. Smith S, Nichols T. Threshold-free cluster enhancement: addressing problems of smoothing, threshold dependence and localisation in cluster inference. Neuroimage 2009;44:83–98. https://doi.org/10.1016/j.neuroimage.2008.03.061.
31. Snider SB, Fischer D, McKeown ME, et al. Regional distribution of brain injury after cardiac arrest: clinical and electrographic correlates. Neurology 2022:98. https://doi.org/10.1212/WNL.0000000000013301.
32. Benjamini Y, Hochberg Y. Controlling the false discovery rate: a practical and powerful approach to multiple testing. J R Stat Soc Ser B Stat Methodol 1995;57:289–300. https://doi.org/10.1111/j.2517-6161.1995.tb02031.x.
33. Sandroni C, Cronberg T, Sekhon M. Brain injury after cardiac arrest: pathophysiology, treatment, and prognosis. Intensive Care Med 2021;47:1393–414. https://doi.org/10.1007/s00134-021-06548-2.
34. De Stefano P, Carboni M, Pugin D, Seeck M, Vulliémoz S. Brain networks involved in generalized periodic discharges (GPD) in post-anoxic-ischemic encephalopathy. Resuscitation 2020;155:143–51. https://doi.org/10.1016/j.resuscitation.2020.07.030.
35. van Putten MJAM, Hofmeijer J. Generalized periodic discharges: pathophysiology and clinical considerations. Epilepsy Behav 2015;49:228–33. https://doi.org/10.1016/j.yebeh.2015.04.007. PubMed PMID: 25944113.
36. Ruijter BJ, Tjepkema-Cloostermans MC, Tromp SC, et al. Early electroencephalography for outcome prediction of postanoxic coma: a prospective cohort study. Ann Neurol 2019;86:203–14. https://doi.org/10.1002/ana.25518.
37. Van Putten MJAM, Ruijter BJ, Horn J, et al. Quantitative characterization of rhythmic and periodic EEG patterns in patients in a coma after cardiac arrest and association with outcome. Neurology 2024;103:e209608. https://doi.org/10.1212/WNL.0000000000209608.

38. Treiman DM, Walton NY, Kendrick C. A progressive sequence of electroencephalographic changes during generalized convulsive status epilepticus. Epilepsy Res 1990;5:49–60. https://doi.org/10.1016/0920-1211(90)90065-4.
39. De Stefano P, Leitinger M, Misirocchi F, Quintard H, Degano G, Trinka E. Myoclonus after cardiac arrest: need for standardization—a systematic review and research proposal on terminology. Crit Care Med 2025;53:e410–23. https://doi.org/10.1097/CCM.0000000000006521.
40. Foley JM, Watson CW, Adams RD. Significance of the electroencephalographic changes in hepatic coma. Trans Am Neurol Assoc 1950;51:161–5.
41. Alkhachroum AM, Al-Abri H, Sachdeva A, et al. Generalized periodic discharges with and without triphasic morphology. J Clin Neurophysiol 2018;35:144. https://doi.org/10.1097/WNP.0000000000000441.
42. Benghanem S, Novy J, Cariou A, Pruvost-Robieux E, Ben-Hamouda N, Rossetti AO. Degree of neurological recovery as a function of initial neuron-specific enolase levels and electroencephalographic patterns in survivors of cardiac arrest: a bicentric study. Resuscitation 2025110757. https://doi.org/10.1016/j.resuscitation.2025.110757.
43. Tziakouri A, Novy J, Ben-Hamouda N, Rossetti AO. Relationship between serum neuron-specific enolase and EEG after cardiac arrest: a reappraisal. Clin Neurophysiol 2023;151:100–6. https://doi.org/10.1016/j.clinph.2023.05.001.
44. Pelle J, Pruvost-Robieux E, Dumas F, et al. Personalized neuron-specific enolase level based on EEG pattern for prediction of poor outcome after cardiac arrest. Ann Intensive Care 2025;15:11. https://doi.org/10.1186/s13613-024-01406-y.
45. Kim YJ, Kim YH, Youn CS, et al. Different neuroprognostication thresholds of neuron-specific enolase in shockable and non-shockable out-of-hospital cardiac arrest: a prospective multicenter observational study in Korea (the KORHN-PRO registry). Crit Care 2023;27:313. https://doi.org/10.1186/s13054-023-04603-6.
46. Wuerz RC, Holliman CJ, Meador SA, Swope GE, Balogh R. Effect of age on prehospital cardiac resuscitation outcome. Am J Emerg Med 1995;13:389–91. https://doi.org/10.1016/0735-6757(95)90120-5.
47. Elmer J, Torres C, Aufderheide TP, et al. Association of early withdrawal of life-sustaining therapy for perceived neurological prognosis with mortality after cardiac arrest. Resuscitation 2016;102:127–35. https://doi.org/10.1016/j.resuscitation.2016.01.016.
48. Calabrese E, Gandhi S, Shih J, et al. Parieto-occipital injury on diffusion MRI correlates with poor neurologic outcome following cardiac arrest. Am J Neuroradiol 2023;44:254–60. https://doi.org/10.3174/ajnr.A7779.
49. Backman S, Cronberg T, Rosén I, Westhall E. Reduced EEG montage has a high accuracy in the post cardiac arrest setting. Clin Neurophysiol Off J Int Fed Clin Neurophysiol 2020;131:2216–23. https://doi.org/10.1016/j.clinph.2020.06.021.